JP2J.8 The Extended GBVTD and the recovery of the tropical cyclones asymmetric structures

Yu-Chieng Liou[1], Tai-Chi Chen Wang[1], Wen-Chau Lee[2], Ya-Ju Chang[1]
[1] Department of Atmospheric Sciences, National Central University, Jhongli City, Taiwan
[2] National Center for Atmospheric Research, Boulder, Colorado, USA

1. Introduction

The Ground Based Velocity Track Display (GBVTD) technique, proposed by Lee et al. (1999) and Lee and Marks (2000), is extended to two Doppler radars to retrieve a tropical cyclone's (TC) asymmetric radial wind component up to its angular wave number one structure. As a result, the accuracy of the retrieved TC tangential wind component can be further improved as well. A comparison with the traditional dual-Doppler synthesis indicates that this Extended GBVTD (EGBVTD) approach is able to estimate more of the TC circulation when there are missing data. The feasibility of the proposed EGBVTD method is demonstrated by applying it to a real case study.

2. The original GBVTD formulation

The geometry and symbols used for the GBVTD after Lee et. al. (1999) with minor modification is plotted in Fig. 1. In the formulation, the horizontal projection of the observed Doppler velocity ($\hat{V}_d$) can be expressed by:

$$\frac{\hat{V}_d}{\cos\phi} = V_M \begin{bmatrix} \cos(\theta_T-\theta_M)\left(\frac{1-\cos\alpha_{\max}}{2}\cos 2\psi + \frac{1+\cos\alpha_{\max}}{2}\right) \\ -\sin(\theta_T-\theta_M)\sin\alpha_{\max}\sin\psi \end{bmatrix} - V_T\sin\psi + V_R\cos\psi \quad (1)$$

where ϕ is the radar elevation angle, θ_T is the angle for the TC center viewed from the radar site, V_M and θ_M are the speed and direction of the mean wind vector ($\vec{V}_M$), respectively. The quantity $\hat{V}_d$, the tangential (V_T) as well as the radial (V_R) wind components of the storm are decomposed by a truncated Fourier series in terms of ψ (see Fig. 1 for definition):

$$\hat{V}_d(\psi)/\cos\phi = \sum_{n=0}^{L}\left(A_n\cos n\psi + B_n\sin n\psi\right) \quad (2)$$

$$V_T(\psi) = V_TC_0 + \sum_{n=1}^{M}\left(V_TC_n\cos n\psi + V_TS_n\sin n\psi\right) \quad (3)$$

$$V_R(\psi) = V_RC_0 + \sum_{n=1}^{N}\left(V_RC_n\cos n\psi + V_RS_n\sin n\psi\right) \quad (4)$$

where ϕ is the radar elevation angle. The coefficients A_n and B_n in (2) can be computed through the curve fitting of the observed Doppler velocities sampled along the analysis ring. Let *L*=3 and *M*=*N*=2, the unknown parameters $V_TC_n(V_RC_n)$ and $V_TS_n(V_RS_n)$ in (3) and (4) are related to the computable coefficients (A_n, B_n) by:

$$V_M\cos(\theta_T-\theta_M) = A_0 + A_2 - V_RC_1 \quad (5)$$

$$V_TC_0 = -B_1 - B_3 - V_M\sin(\theta_T-\theta_M)\times\sin\alpha_{\max} \quad (6)$$

$$V_RC_0 = A_1 + A_3 - V_RC_2 \quad (7)$$

$$V_TS_1 = A_2 - A_0 + (A_0 + A_2 - V_RC_1)\times\cos\alpha_{\max} \quad (8)$$

$$V_TC_1 = -2B_2 + V_RS_1 \quad (9)$$

$$V_TS_2 = 2A_3 - V_RC_2 \quad (10)$$

$$V_TC_2 = -2B_3 + V_RS_2 \quad (11)$$

Lee et al. (1999) further neglected the V_R at higher wave numbers (i.e. V_RC_n and V_RS_n, $n\geq 1$) in order to close the equations (5)-(11). As a result, the GBVTD-retrieved products include the TC tangential winds (angular wave numbers zero and higher), and the axisymmetric part of the radial winds (V_RC_0). Furthermore, the mean tangential wind (V_TC_0) is contaminated by $V_M\sin(\theta_T-\theta_M)$ in (6). The existing information is not sufficient to make a further separation of V_M and θ_M.

3. The EGBVTD approach

Figure 2 illustrates the applications of the GBVTD method to two radar systems, represented by radar A and radar B, respectively. In addition, the formulations listed in (5)-(11) are slightly modified by retaining the parameters relevant to the wave number one structure of the TC radial winds (i.e. V_RC_1, V_RS_1).

3.1 Estimation of the mean flow V_M and θ_M

Since V_TC_0 in (6) represents the axisymmetric portion of the tangential velocity, the estimations of V_TC_0 by radar A and radar B ought to be the same. This leads to the following expression:

$$J = \sum_{i=1}^{N}\left\{\left[-B_1 - B_3 - V_M\sin(\theta_T-\theta_M)\sin\alpha_{\max}\right]_i - \left[-B_1' - B_3' - V_M\sin(\theta_T'-\theta_M)\sin\alpha_{\max}'\right]_i\right\}^2 \quad (12)$$

where the terms with a prime stand for the coefficients computed or viewed from radar B, and *N* is the number of analysis rings locating at the same altitude, the subscript *i* is the index of each ring. Now, for each layer, within a pre-determined range, we seek a set of optimal V_M and θ_M, which minimizes (12). The above description demonstrates the procedure proposed for extracting information about the mean flow by applying the GBVTD method to data from two Doppler radars.

3.2 Derivation of the asymmetric TC radial wind structure

After V_M and θ_M are known, equation (5) can be used to derive $V_R C_1$. Then, using P_2 in Fig. 2 as an example, we apply equation (1) at P_2, but using the data collected by radar B. Since the value of ψ' at P_2 is π, (1) can be simplified to the following form:

$$\frac{\hat{V}_d'(P_2)}{\cos\phi'} = V_M \cos(\theta_T' - \theta_M) - V_R(P_2) \quad (13)$$

Since $\hat{V}_d'(P_2)$ can be measured by radar B at P_2, one can derive $V_R(P_2)$, or the total TC radial wind at this point.

The next step is to expand $V_R(P_2)$ using the ψ angle system viewed from radar A to yield:

$$V_R(P_2) = V_R C_0 + V_R C_1 \cos\psi_2 + V_R S_1 \sin\psi_2 \quad (14)$$

where ψ_2 is the value of angle ψ at P_2, viewed from radar A. Since $V_R C_0$ and $V_R C_1$ are already estimated from (7) and (5), respectively, the only unknown variable $V_R S_1$ in (14) can finally be solved. This set of coefficients $V_R C_0$, $V_R C_1$ and $V_R S_1$ specifies the mean as well as the wave number one structure of the TC radial flows along the given analysis ring. Moreover, it is also found that a better retrieval of the wave number one structure of the TC tangential flow can also be achieved by inserting the newly derived $V_R C_1$ and $V_R S_1$ into (8) and (9) to improve the accuracy of $V_T S_1$ and $V_T C_1$.

4. A real case study – Typhoon Nari (2001)

4.1 The mean wind in Nari's inner core

We have tested a series of experiments using idealized TC wind fields produced by a Rankine vortex model, and the results are rather satisfactory. In this section, we only presented the results from a real case study. Typhoon Nari struck Taiwan on 16 September 2001 and caused extremely serious damage. Figure 3 shows the geographic locations of the CAA and RCWF radar systems in northern Taiwan, and the storm center of Nari. Figure 4 depicts the storm track and the retrieved mean winds in Nari's inner core at five different heights. The speeds of the storm's movement at these five layers are approximately between 6.0 and 8.0 ms^{-1}, and the directions vary from 235^0 to 250^0. A vertical, mass-weighted averaging of the storm movements at different layers results in a northeasterly mean storm track, with the speed and direction equal to 6.7 ms^{-1} and 244^0, respectively (shown by a thick arrow in Fig. 4). From 3.0 km to 6.0 km, the direction of the retrieved mean wind turns counterclockwise, from approximately 191^0 to 291^0. Below (above) 3.75 km, the mean wind tends to deviate to the right (left) of the storm track. A mass-weighted averaging throughout these five layers is also conducted for the retrieved mean wind. The resulting averaged mean wind speed is 5.0 ms^{-1}, and the direction is 250^0, which shows a slight leftward deviation from the average storm track. This result is consistent with the findings of Marks et al. (1992) in which the structures of Hurricane Norbert (1984) was investigated by an airborne Doppler radar.

4.2 The mean wind-relative intrinsic typhoon circulation

Figures 5 and 6 illustrate Nari's mean wind-relative intrinsic radial and tangential wind structures at 6.0 km, respectively. It can be seen that there is an inflow (outflow) taking place in the east-southeast (north-northwest) quadrant of the typhoon, and a strong (weak) tangential wind region located in the northeast (southwest) portion of the typhoon. The peak wind speed in the northeast exceeds 25.0 ms^{-1}. These results are similar both qualitatively and quantitatively to those obtained from the dual-Doppler synthesis (not shown).

The Nari radial wind at Z=3.0 km derived by dual-Doppler analysis is displayed in Fig. 7. Due to the limited data overlap for both radar systems, and the incomplete data coverage surrounding the typhoon center, the traditional dual-Doppler approach can only generate a ground-relative wind field in the storm's northern quadrant within a relatively small area. However, the EGBVTD method is still capable of recovering a complete typhoon circulation structure over a much larger domain, as described by Fig. 8. The reason is that the method of curve fitting used in EGBVTD does not require a full radar data coverage over the entire analysis ring. In other words, even with missing radar data, the EGBVTD method can still separate the storm from the mean flow, and resolve the intrinsic TC asymmetric flow structures. An estimation using idealized Rankine vortex model indicates that the quality of the EGBVTD retrievals remains satisfactory even when the length of the missing data gap along a given analysis ring reaches approximately 120^o, or 1/3 of the complete data coverage. This is considered an advantage of the EGBVTD over the tradition dual-Doppler method.

5. Summary

The major improvement achieved by this so-called EGBVTD approach is that the asymmetric structures of the TC radial winds can be separated from the mean wind and retrieved with substantial success, and the accuracy of the retrieved tangential winds can also be improved accordingly. Although two radars are needed, a comparison with the traditional dual-Doppler synthesis indicates that the advantages of this EGBVTD method are: (1) it is possible to estimate the mean wind and isolate the storm circulation when the radar data coverage surrounding the TC center is incomplete; (2) the requirement for overlapping data from two radars along a given analysis ring is less. This implies that the EGBVTD retrieval can be performed over a larger domain than that of dual-Doppler synthesis.

6. References

Lee W.-C., B. J.-D. Jou, P.-L. Chang, and S.-M. Deng, 1999: Tropical cyclones kinematic structure retrieved from single-Doppler radar observations, Part I: Interpretation of Doppler velocity patterns and the GBVTD technique, *Mon. Wea. Rev.*, **127**, 2419-2439.

_____, and F. D. Marks, 2000: Tropical cyclones kinematic structure retrieved form single-Doppler radar observations, Part II: The GBVTD-simplex center finding algorithm, *Mon. Wea. Rev.*, **128**, 1925-1936.

Marks, F. D., R. A. Houze and J. F. Gamache, 1992: Dual-aircraft investigation of the inner core of Hurricane Norbert, Part I: Kinematic structure, *J. Atmos. Sci.*, **49**, 919-942.

Acknowledgement. This research is supported by the National Science Council of Taiwan under NSC 93-2625-Z-008-014, NSC 93-2111-M-008-024-AP3.

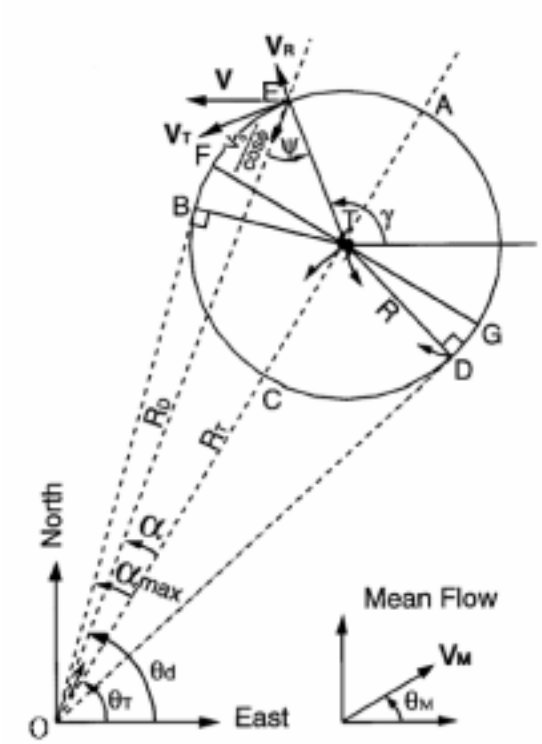

Fig 1 The geometry and symbols of GBVTD (from Lee et. al. 1999).

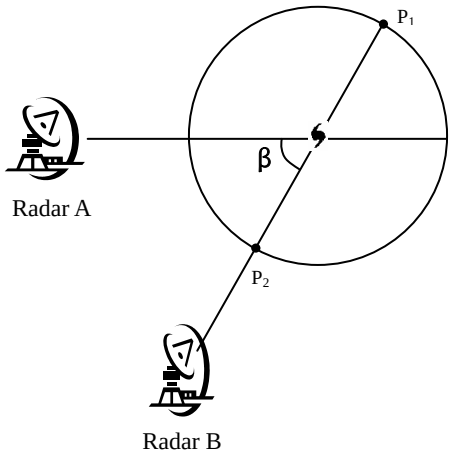

Fig 2 The geometry of EGBVTD. The angle β is the difference of the radar viewing angle from radar sites A and B toward the TC center, which is represented by a typhoon symbol.

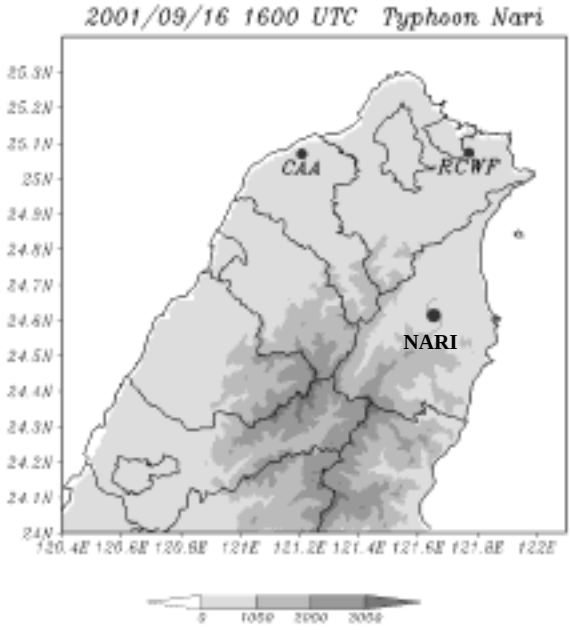

Fig 3 The geographic locations of Doppler radars CAA and RCWF in northern Taiwan. The typhoon symbol depicts the location of typhoon Nari's center at the analysis hour. The shading represents the terrain height in meters above sea level (ASL).

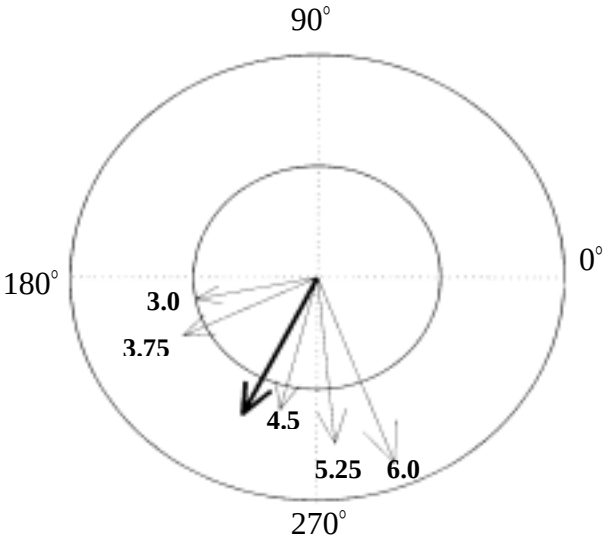

Fig 4 Magnitude and direction of the storm track and the retrieved mean wind. The thick arrow denotes the vertical, mass-weighted averaged storm track. The thin arrows illustrate the EGBVTD-derived mean winds within the inner core region for five different layers. The wind speeds are represented by the circles. The numbers at the tip of the thin arrows represent the height, ranging from 3.0 km to 6.0 km.

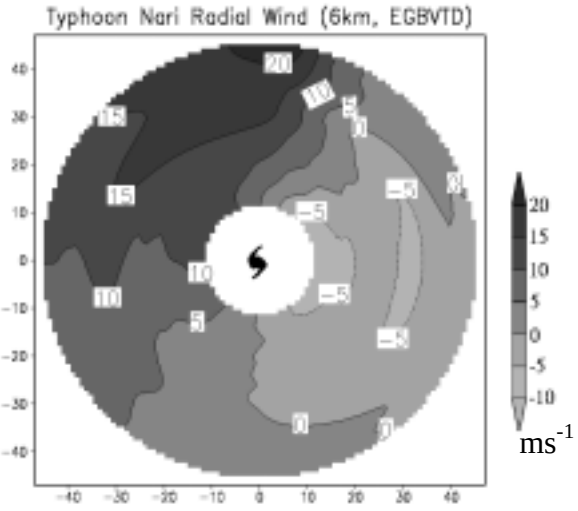

Fig 5 The mean-wind relative radial wind field of typhoon Nari at Z=6.0 km, derived by EGBVTD. The wind fields are shaded at intervals of 5.0 ms^{-1}. The storm center is indicated by a typhoon symbol.

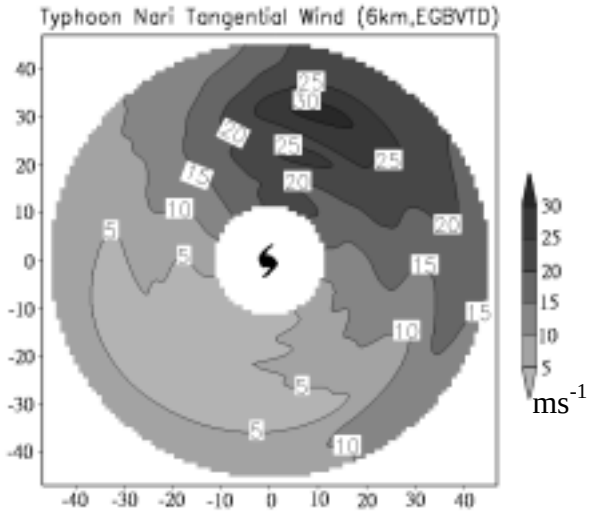

Fig 6 Same as in Fig. 5, but for the mean-wind relative tangential wind fields.

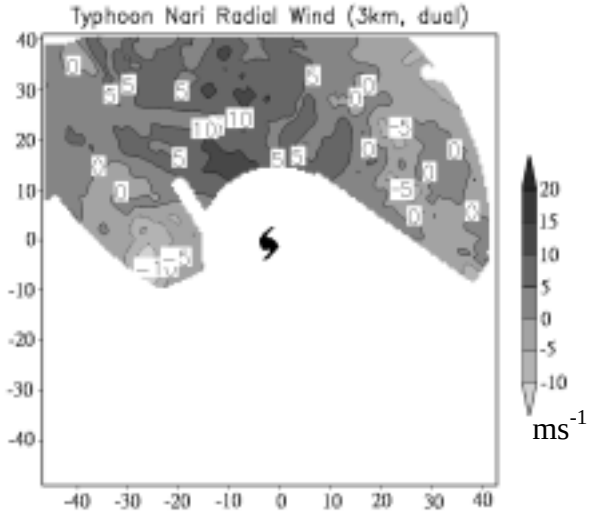

Fig 7 The radial wind field of typhoon Nari at Z=3.0 km, derived by traditional Dual-Doppler synthesis. The wind fields are shaded at intervals of 5.0 ms^{-1}.

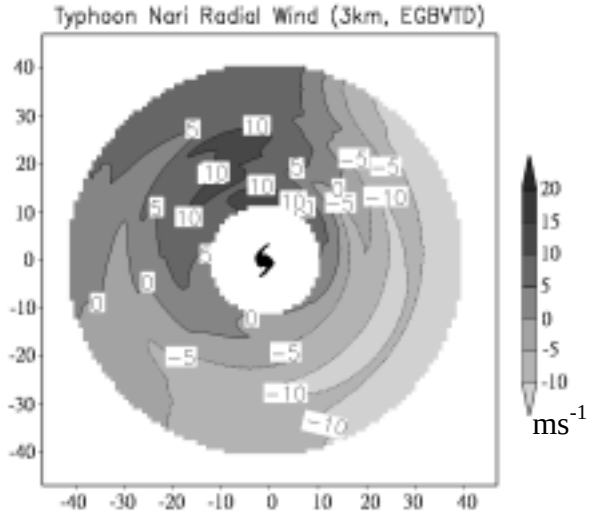

Fig 8 Same as in Fig. 7, but is the result derived from EGBVTD method..